On the Scattering Function of Simple Fluids in Finite Systems

M. Malek Mansour,[1,2] **A. L. Garcia,**[1,2] **J. W. Turner,**[1] **and M. Mareschal**[1]

The density–density dynamical correlation function of a simple fluid in a finite container subject to a constant temperature difference is explicitly obtained. In small systems, such as those realized in computer experiments, new peaks appear in the scattering spectrum, even at equilibrium, arising from standing waves produced by the fluctuations. Away from equilibrium, these peaks are asymmetric in the same manner as the Brillouin lines. The macroscopic limit is also considered and the correction to the usual "infinite system approximation" is explicitly obtained.

1. INTRODUCTION

Some years ago it was realized that nonequilibrium modifications to the dynamical correlation functions for hydrodynamic fluctuations were measurable by light scattering experiments.[1–3] Yet, in contrast to the wealth of theoretical treatments of the problem (refs. 4–8; see ref. 9 for a recent review), there remains a paucity of experimental results, due to the numerous complications arising when performing small-angle scattering experiments.[10–12] Another promising approach is by direct computer simulation of an out-of-equilibrium system, such as a fluid subjected to a constant temperature difference.[13],3 Using stochastic particle simulations based on the Boltzmann equation,[15] nonequilibrium modifications to the static correlation functions have been measured for a dilute gas[16,17] (see

---

[1] Université Libre de Bruxelles, Faculté des Sciences, B-1050 Brussels, Belgium.
[2] Center for Statistical Mechanics and Thermodynamics, University of Texas at Austin, Austin, Texas 78712.
[3] See ref. 14 for a recent review of particle simulations used in the study of nonequilibrium systems.

also ref. 18). Thus, a new influx of data from computer experiments is stimulating renewed interest in analytical work.

The theoretical aspects of the problem, as relevant to computer experiments, present some interesting features. The finite-size (or geometrical) effects are in general as important as the dynamical effects and consequently the boundary value problem must be considered with great care. This precludes some of the usual approximations developed for macroscopic systems.[9] Furthermore, since the system is typically closed, the conservation of total particle number plays an equally important role. These effects have been considered before, since they do influence the light scattering results.[19–21] In particular, the general form of the nonequilibrium scattering function for a liquid with vanishing thermal expansivity coefficient has been obtained by Satten and Ronis.[20] This expression proves to be quite complicated and one is unfortunately reduced to numerical evaluation. In nonequilibrium light scattering experiments only the integrated scattering amplitude is observable, so obtaining a simple expression for the full scattering function has not been important (a nice derivation of the integrated spectrum is presented in ref. 21). This is not the case for computer experiments where the entire line shape can be measured. It is therefore highly desirable to simplify the general expression in order to explain the measured spectrum in terms of simple physical processes.[4] This is the main purpose of this paper and is presented in Section 3. In Section 4, we also discuss limiting forms of the scattering function for various macroscopic regimes. In particular, corrections to the usual "infinite system approximation" are presented.

2. BASIC EQUATIONS

A common theoretical approach for obtaining the scattering function is the Landau–Lifshitz fluctuating hydrodynamics formalism,[22] mainly because of its relative simplicity as compared with more fundamental approaches.[3,8] As such, we restrict our attention to fluctuation phenomena on hydrodynamic scales rather than atomic scales (which are more suitably treated by kinetic theory). In this paper we apply this formalism to a simple fluid model with the following characteristics:

1.   The thermal expansion coefficient is zero (water at 4°C and normal fluid liquid helium near the λ point satisfy this condition).

2.   The transport coefficients and the sound speed are constants, independent of temperature.

---

[4] So far this program has been achieved only for systems where the boundary effects are neglected.[9]

By the first assumption, the momentum equation is decoupled from the energy equation and in turn yields a constant macroscopic density throughout the system.[2,6] While these assumptions considerably simplify the analysis, it is known that the main physical aspects of the problem are preserved.[9] The detailed analysis, including the effect of an imposed strain and the evaluation of all the various static and dynamic correlation functions, is quite lengthy and has been presented elsewhere.[23] In this paper, we calculate the dynamic density–density correlation function, which is commonly measured in molecular dynamics simulations. In light scattering experiments this function is associated with the scattered spectrum.[24]

The fluid is confined between two parallel planes located at $y = 0$ and $y = L$, which act as infinite reservoirs, so that by fixing their temperatures one can impose the desired heat flux across the system. The two boundaries perpendicular to these walls are taken as periodic boundaries (this construction is typical for computer simulations[13]). As can be easily checked from the macroscopic hydrodynamic equations, at the stationary state the pressure is constant, the velocity is zero, and the temperature is a linear function of the imposed gradient (note that there is no instability because we do not consider external fields in our formulation[25]).

To study the fluctuations, we first linearize the fluctuating hydrodynamic equations around the macroscopic reference state. Since we are mainly interested in the influence of the nonequilibrium constraint and since we have periodic boundary conditions in the x and z directions, we limit ourselves to reduced variables defined by

$$\delta h(y) = \frac{1}{S} \int_0^{L_x} dx \int_0^{L_z} dz \, \delta h(x, y, z) \tag{1}$$

where $S = L_x L_z$ is the wall cross section and δh is the fluctuation of the hydrodynamic quantity h. In computer experiments, the system is typically divided into a set of parallel cells and the quantities measured are precisely the reduced variables. Our use of reduced variables is equivalent to setting the "parallel" Fourier components of the hydrodynamic variables to zero, which considerably simplifies the analysis. It is easy to check that the reduced equations for the x and z components of the velocity fluctuations decouple from the other variables and are not influenced by the constraint. We will therefore concentrate our attention on the remaining equations for the mass density $\delta \rho$ and the y component of the velocity δv,

$$\frac{\partial}{\partial t} \delta \rho = -\rho_0 \frac{\partial}{\partial y} \delta v \tag{2}$$

$$\frac{\partial}{\partial t} \delta v = -\alpha \frac{\partial}{\partial y} \delta \rho + \frac{1}{\rho_0} \left(\frac{4\eta}{3} + \zeta \right) \frac{\partial^2}{\partial y^2} \delta v + \frac{1}{\rho_0} \frac{\partial}{\partial y} F(y, t) \tag{3}$$

where the subscript 0 refers to macroscopic quantities, η and ζ are the shear and bulk viscosity coefficients, and $\alpha = (\partial P_0/\partial \rho_0)_{T_0}/\rho_0$. The random component of the stress tensor $F(y, t)$ is a white noise process in space and time; it is zero on average and has a correlation[22]

$$\langle F(y, t) F(y', t') \rangle = 2[k_B T_0(y)/S](4\eta/3 + \zeta) \delta(y - y') \delta(t - t') \quad (4)$$

where k_B is the Boltzmann constant and $T_0(y)$ is the macroscopic temperature profile, $T_0(y) = T_0(y = 0) + \gamma y$. Since the fluctuating stress tensor is a function of the local temperature, the nonequilibrium effects in this model arise from the inhomogeneous distribution of Langevin sources.

If we now we assume that the total volume of the system is fixed (not fluctuating), then the boundary condition for δv follows from the conservation of total mass:

$$\int_0^L dy \, \delta\rho(y, t) = 0 \Rightarrow \rho_0 \, \delta v(y) \Big|_{y = 0, L} = 0 \quad (5)$$

(i.e., the boundary acts as a rigid wall).[5] No boundary condition for $\delta\rho$ is required, since its evolution is entirely specified by the initial conditions for $\delta\rho$ and δv plus the boundary conditions for δv. From a physical point of view, this reflects the fact that the walls can only constrain the velocity and the temperature, but the density is governed by the internal dynamics of the fluid. The full mathematical aspects of this problem are reported elsewhere.[23] Interestingly, we note that simply requiring that the total volume be fixed specifies entirely the boundary value problem for reduced variables.

From the above geometry and boundary conditions, it is easy to check that the eigenfunctions associated with our evolution equations (2) and (3) are simply $\cos(k\pi y/L)$ for $\delta\rho$ and $\sin(k\pi y/L)$ for δv. We therefore expand the solution as

$$\delta\rho(y, t) = \sum_{k=1}^{\infty} \delta\rho_k(t) \cos\frac{k\pi y}{L}; \qquad \delta\rho_0(t) = 0 \quad (6a)$$

$$\delta v(y, t) = \sum_{k=0}^{\infty} \delta v_k(t) \sin\frac{k\pi y}{L} \quad (6b)$$

---

[5] In computer simulations the containing walls are strictly rigid. The wall is a fixed plane and the particle's velocity is changed the instant it touches the wall. Typically, the particle is thermalized, so that its velocities before and after striking the wall are entirely uncorrelated. In this way, the wall also acts as perfectly conducting, no-slip boundary. This boundary condition on $\delta u_{\parallel}$ and δT, however, is unnecessary for the problem considered in this paper. Our previous studies have discussed the appropriateness of the above boundary conditions when considering computer experiments with thermalizing boundaries.[17,26]

Taking the Fourier transform in time, after some algebra one finds

$$\langle \delta\rho_k(\omega)\, \delta\rho_{k'}(\omega')\rangle = \frac{4k_{\mathrm B}\,\Gamma\rho_0\delta(\omega+\omega')}{\pi V(c^4+4\omega^2\Gamma^2)}\; T_{k,k'}\frac{k^2}{k^2-z^2}\frac{k'^2}{k'^2-z^{*2}} \qquad (7)$$

where V is the total volume of the system, $c=(\alpha\rho_0)^{1/2}$ is the (isothermal) sound speed, $\Gamma=(4\eta/3+\zeta)/2\rho_0$ is the sound attenuation coefficient, and

$$z^2 = \frac{\omega^2 L^2(c^2+2i\omega\Gamma)}{\pi^2(c^4+4\omega^2\Gamma^2)} \qquad (8)$$

The function $T_{k,k'}$ is defined as

$$T_{k,k'} = \frac{1}{2L}\int_0^L dy \cos\frac{k\pi y}{L}\cos\frac{k'\pi y}{L}\,T_0(y) \qquad (9)$$

Although Eq. (7) completes the solution for the density correlation function, the physical aspects are hidden in its present form. To proceed, we must either transform back to real space to obtain $\langle \delta\rho(y,t)\,\delta\rho(y',t')\rangle$ or, better, compute the scattering function, defined as[27]

$$S_q(\omega) = (V/\rho_0 m)(1/L^2)\int_0^L dy \int_0^L dy'\, \exp[i2\pi q(y-y')/L]$$

$$\times \int_{-\infty}^{\infty} d\omega'\, \langle \delta\rho(y,\omega)\,\delta\rho(y',\omega')\rangle \qquad (10)$$

where m is the particle mass. In this paper we focus on the properties of the scattering function $S_q(\omega)$. Note that in computer experiments this function is equivalent (at hydrodynamic scales) to the Fourier transform in time of the Van Hove total correlation function,[27]

$$G_q(t) = \frac{1}{N}\left\langle \sum_{a=1}^{N} \exp[i2\pi q\,\mathbf{1}_y\cdot\mathbf{r}_a(t)/L] \sum_{b=1}^{N} \exp[-i2\pi q\,\mathbf{1}_y\cdot\mathbf{r}_b(t=0)/L]\right\rangle$$

$$(11)$$

where $\mathbf{r}_a$, $\mathbf{r}_b$ are the positions of particles a and b, respectively, $\mathbf{1}_y$ is the unit vector in the y direction, and N is the total number of particles in the system. The scattering function $S_q(\omega)$ is obtained in light scattering from the measured spectrum.[24] In the limit of large equilibrium systems, where the boundary effects may be neglected, the scattering function can be directly obtained from (7) by the replacement $k \to 2q$, $k' \to -2q$. In finite systems, however, there is no similar simple step; we must first obtain the density fluctuations in real space and compute $S_q(\omega)$ from Eq. (10).

In our definition for $S_q(\omega)$, we integrate over the entire space (from $y = 0$ to L) and do not use a weighting function or "beam shape" function. It might appear that this is the origin of our finite-size effects, yet the analysis of Satten and Ronis[20] demonstrated that even if the scattering subvolume is small, boundary effects are significant in nonequilibrium light scattering experiments when the sound attenuation length is comparable to the container dimensions. In computer simulations with containing walls (i.e., not periodic boundary conditions), the boundary effects are always important, even if only a subvolume of the system is considered. Typically, however, the entire system is used to minimize the statistical errors.

Following the above discussion, one finds after some tedious calculations

$$
S_q(\omega) = \frac{32k_B T_a}{\pi m c^4} \frac{\Gamma q^2}{(\omega^2 L^2/\pi^2 c^2 - 4q^2)^2 + 64q^4\omega^2\Gamma^2/c^4}
$$

$$
\times \operatorname{Re} \left\{ q^2 + \frac{4q^2}{\pi(4q^2 - z^2)} z \tan \frac{\pi z}{2} \right.
$$

$$
+ \frac{|z|^2}{4\pi |\cos(\pi z/2)|^2} \left(\frac{\sin[\pi(z - z^*)/2]}{z - z^*} - \frac{\sin[\pi(z + z^*)/2]}{z + z^*} \right)
$$

$$
\left. + \frac{\gamma L}{T_a} q \frac{iz^2}{\pi(4q^2 - z^2)} \left(1 + \frac{2(z^2 + 4q^2)}{\pi z(4q^2 - z^2)} \tan \frac{\pi z}{2} \right) \right\} \qquad (12)
$$

where T_a and γ are the (space) averaged temperature and the temperature gradient, respectively. It should be understood that the above result is not new. It may be obtained from the formulation of Satten and Ronis[20] or that of Schmitz and Cohen[21] restricted to reduced variables and perfectly rigid walls. Before discussing our main contribution, let us plot $S_q(\omega)$ for the range of parameters appropriate to computer experiments. We present the exact solution (12) for thermodynamic equilibrium (i.e., $\gamma = 0$) in Fig. 1 and a nonequilibrium case in Fig. 2 (in each case $q = 1$). Besides the usual Brillouin lines,[24] one also sees two sharp peaks at lower frequency. The location of these extra peaks is found to be at $\omega L/c$ (independent of the harmonic number q). Although it is clear that the extra peaks arise entirely from the influence of the boundary, it is impossible to understand much about their nature from the exact expression (12). At this point, one could argue that it is possible to obtain $S_q(\omega)$ numerically by solving the full hydrodynamic equations, without any approximation,[17,26] thus casting some doubt on the usefulness of the above analysis. Yet the formal expression (12) is useful if we can obtain from it simple limiting forms of $S_q(\omega)$ for the various regimes of interest.
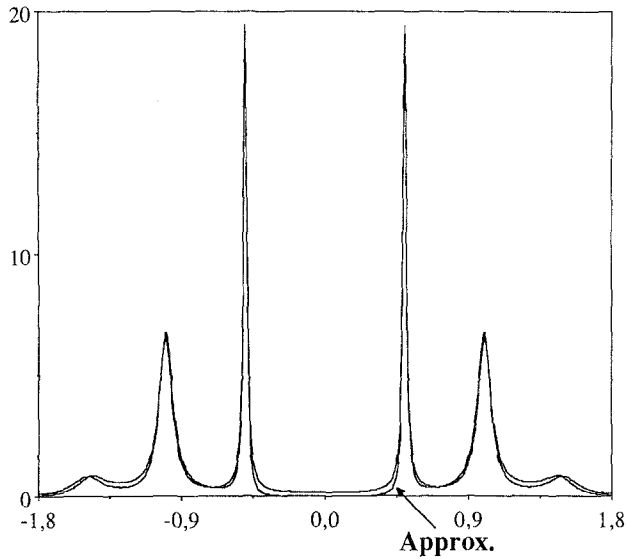
Fig. 1. The scattering function $S_q(\omega)$ as a function of frequency for $q = 1$ and $\gamma = 0$ (equilibrium). The parameters are taken so as to correspond to those used in the computer experiment described in ref. 17: $L = 50$ mean free paths (mfp), $\varepsilon = 5.1 \times 10^{-2}$, $2k_B T_a \Gamma/m\pi c^4 = 8.46 \times 10^{-2}$, $\rho_0 = 400$ particles per (mfp)^3. Both the exact solution [Eq. (12)] and the approximate solution [Eq. (14)] are shown.
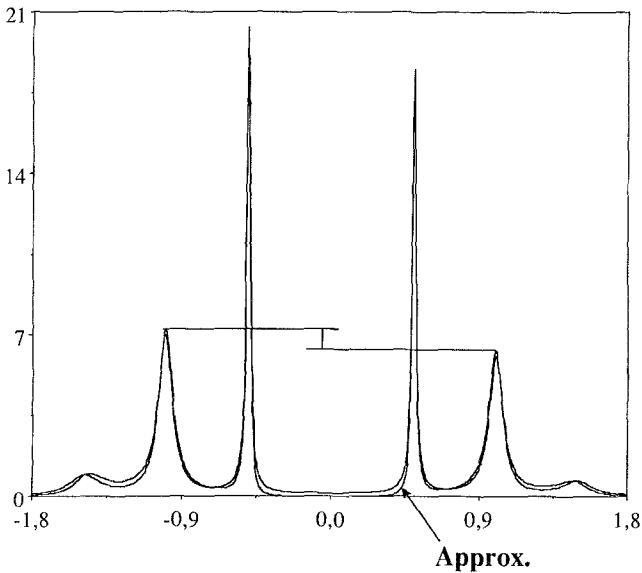

Fig. 2. The scattering function $S_q(\omega)$ as a function of frequency for $q = 1$ and $\gamma L/T_a = 4/3$ (nonequilibrium), $2k_B T_a \Gamma/m\pi c^4 = 6.91 \times 10^{-2}$. See caption to Fig. 1 for details.

3. SCATTERING FUNCTION IN COMPUTER EXPERIMENTS

We start by introducing the dimensionless parameters $\tilde{\omega}$ and ε as

$$\tilde{\omega} = \frac{\omega}{(2\pi q/L)c}; \qquad \varepsilon = \frac{\Gamma}{c}\frac{2\pi q}{L} \tag{13}$$

with the restrictions $\tilde{\omega} \approx o(1)$ and $\varepsilon \ll 1$. The latter condition must be fulfilled in order to remain in the hydrodynamic regime.[24] With the above requirements, it is possible to simplify considerably the expression (12). This involves matching Pade-like approximations around the various peaks and the final result depends crucially on the allowed values of q.

In this section we consider $S_q(\omega)$ in the limit of small q (typically $q = 1$ or $q = 2$). In computer experiments the wavelength (L/q) on which the dynamic correlations are measured will have to be of the order of the system size if one wishes to remain in the hydrodynamic regime (ε between 10^{-1} and 10^{-2} for $q = 1$). Moreover, the statistical error in the data constrains one to consider only the zero wavenumber in the parallel direction (i.e., reduced variables). The limit we are using is thus appropriate for comparison with particle simulations. Under these restrictions, one finds after some algebra

$$S_q(\omega) = \frac{2k_{\mathrm{B}} T_a \Gamma}{m\pi c^4} \frac{\tilde{\omega}^2}{\cos(2\pi q\tilde{\omega}) + 1 + 2\pi^2 q^2 \varepsilon^2 \tilde{\omega}^4} \frac{1}{(\tilde{\omega}^2 - 1)^2 + 4\tilde{\omega}^2 \varepsilon^2}$$

$$\times \left\{ 1 - \frac{2L\gamma}{q\pi T_a} \frac{\tilde{\omega}\varepsilon}{(\tilde{\omega}^2 - 1)^2 + 4\tilde{\omega}^2\varepsilon^2} \right.$$

$$\left. \times \left[\frac{1}{2}(\tilde{\omega}^2 + 1)[1 - \cos(2\pi q\tilde{\omega})] + \frac{2}{3}\pi^2\varepsilon^2 q^2\tilde{\omega}^2 - \frac{1}{3}\sin^2(2\pi q\tilde{\omega}) \right] \right\} \tag{14}$$

The front factor represents the equilibrium contribution. The term $[(\tilde{\omega}^2 - 1)^2 + 4\tilde{\omega}^2\varepsilon^2]^{-1}$ yields the Brillouin lines; its maxima are at $\tilde{\omega} = \pm 1$. The term $[\cos(2\pi q\tilde{\omega}) + 1 + 2\pi^2 q^2\varepsilon^2\tilde{\omega}^4]^{-1}$ reflects the finite-size effect and is responsible for the extra peaks that occur for $\tilde{\omega} = \pm 1/2q, \pm 3/2q,...$. The absence of terms nonlinear in the temperature gradient γ is a result of the two assumptions that are the basis of our fluid model (see Section 2); for the same reason, we have no Rayleigh line. In Figs. 1 and 2 we see that the approximation is already quite good, at least near the peaks, for the parameters of the computer simulation described in ref. 17 ($\varepsilon \approx 5 \times 10^{-2}$). Note that an alternative, but somewhat more cumbersome, approximation has already been provided in ref. 17.

The nonequilibrium terms are odd in frequency, yielding the asymmetry seen in Fig. 2. The part corresponding to the Brillouin lines is a

double Lorentzian, in agreement with previous calculations where the boundary effects are neglected.[9] Its coefficient, however, is different as a direct result of the influence of the boundaries. To see this, let us consider in more detail the origin of the asymmetry in the spectrum. Satten and Ronis[20] found a modulation of the Brillouin lines because of the boundary effect and a smaller asymmetry than that obtained in calculations where the boundary effects were neglected. In our limit, the finite-size peaks do not overlap with the Brillouin lines, but are well separated. Yet a detailed analysis of the various terms in the exact expression (12) shows that the asymmetry arises mainly from the finite-size effect. Consider, for instance, the nonequilibrium contribution $S_q^{ne}(\omega)$, which, from the exact expression, may be written as the product of two terms:

$$S_q^{ne}(\omega) = \frac{32 k_B T_a}{\pi m c^4} \frac{\Gamma q^2}{(\omega^2 L^2/\pi^2 c^2 - 4q^2)^2 + 64q^4\omega^2\Gamma^2/c^4}$$

$$\times \operatorname{Re}\left[\frac{\gamma L}{T_a} q \frac{iz^2}{\pi(4q^2 - z^2)}\left(1 + \frac{2(z^2 + 4q^2)}{\pi z(4q^2 - z^2)}\tan\frac{\pi z}{2}\right)\right] \quad (15)$$

The first term is the usual Lorentzian responsible for the Brillouin lines, while the second contains all the nonequilibrium effects. As seen in Fig. 3,
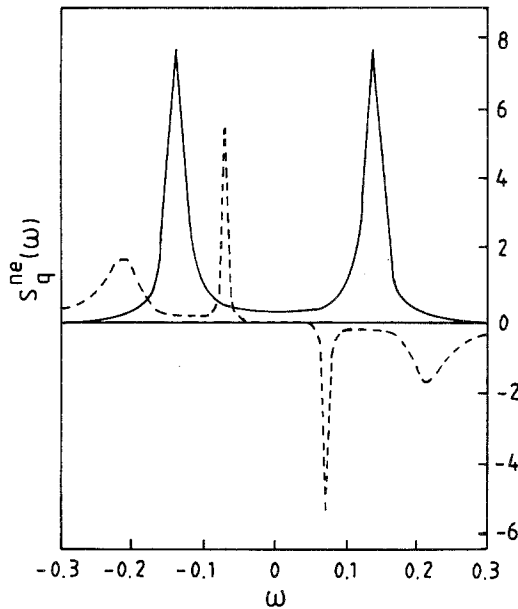

Fig. 3.   (—) The first and (- -) second terms of the nonequilibrium contributions to the scattering functions $S_q^{ne}(\omega)$ [see Eq. (15)]. The first term is a Lorentzian with maxima at $\omega L/c = \pm 2\pi$. Note that the maxima of the second term are at $\omega L/c = \pm\pi, \pm 3\pi,\dots$.

where each of the terms is depicted, the second term has extrema located at $\omega L/c = \pm\pi$, $\pm 3\pi,...$, i.e., at the locations of the finite-size peaks. The origin of the asymmetry in the Brillouin lines seems therefore to be dominated by the boundary effects, at least for the range of parameters we are considering. For macroscopic systems, such as laboratory systems used in light scattering experiments, the interplay between bulk and boundary effects will be different. Though nonlinear effects are not considered in our analysis,[28] for computer experiments, due to the small system size and the presence of reflecting boundaries, the finite-size effect seems to dominate over nonlinear effects even though the imposed nonequilibrium constraints are extremely large (see ref. 21 for more details).

Consider now the finite-size peaks; an obvious explanation for the extra lines at odd values of $\omega L/\pi c$ is the existence of stationary sound waves across the system, as originally suggested in ref. 19 for equilibrium systems and later remarked in ref. 20 for nonequilibrium systems. The density fluctuations are converted to sound waves, which are reflected by the rigid walls, giving rise to stationary waves. For this picture to be consistent, however, we have to check two consequences. First, for a system with periodic boundary conditions in the y direction, the extra peaks must disappear, since for the stationary waves to be formed, one needs coherent sound waves crossing. It is easy to check theoretically that this is indeed so. It is also known from equilibrium computer simulations measurements that there are no such peaks (some other effects can, however, be observed if the time correlation functions are considered for lag times greater than the sound crossing time in the system[29]).

Next, the perpendicular current static correlation function must obviously contain this effect. At equilibrium this function is delta-correlated. The random distribution of the phases of the Langevin sources ensures time-reversal symmetry and thus eliminates any observable effect in this function. In nonequilibrium systems, however, the average amplitudes of the Langevin sources are not equal and the standing waves produce an observable effect. To see this, consider the (perpendicular) velocity–velocity static correlation function, which is given by

$$\langle \delta v(y)\, \delta v(y') \rangle_{\text{st}} - \frac{k_{\text{B}} T_0(y)}{\rho_0 S} \delta(y - y')$$

$$= \sum_{\substack{k+k' \text{ odd}}}^{\infty} \sum^{\infty} \sin\frac{k\pi y}{L} \sin\frac{k'\pi y'}{L}$$

$$\times \frac{16 k_{\text{B}} \gamma k k'}{\rho_0 S \pi^2 [(k^2 - k'^2)^2 + 8\pi^2 \varepsilon^2 k^2 k'^2 (k^2 + k'^2)]} \tag{16}$$

The term on the rhs is the nonequilibrium contribution; it is plotted in Fig. 4 for various values of L. Its form clearly suggests the existence of spatially damped standing waves across the system. In order to be sure, however, we have to compute the asymptotic behavior of (16) in the limit $L \to \infty$ ($\varepsilon \to 0$). For the sake of simplicity, we set

$$y'/L = 1/2, \qquad y/L = 1/2 + r \qquad (-1/2 \leqslant r \leqslant 1/2) \qquad (17)$$

and limit ourselves to the study of the function

$$g_{vv}(r) \equiv \langle \delta v(y = L/2 + Lr)\, \delta v(y' = L/2)\rangle - \frac{k_B T_0(r)}{\rho_0 V} \delta(r) \qquad (18)$$

which represents the nonequilibrium part of (16) evaluated with respect to the center of the system. To dominant order in ε one finds (see ref. 23 for details)

$$g_{vv}(r) \approx (-k_B \gamma/2\pi^{1/2}\rho_0 S)\, r\varepsilon^{-1/2} \exp(-r\varepsilon^{-1/2}\pi^{1/2}/2) \sin(r\varepsilon^{-1/2}\pi^{1/2}/2 + \pi/4) \qquad (19)$$

Clearly, for any given value of r, the nonequilibrium contribution to the static velocity autocorrelation function behaves as $O(\exp\{-1/\sqrt{\varepsilon}\})$ and therefore vanishes exponentially with the system size L. On the other hand, for fixed L, the above correlation function is significantly different from zero only for $|r| \sim O(\sqrt{\varepsilon})$. The correlation length is therefore of the order
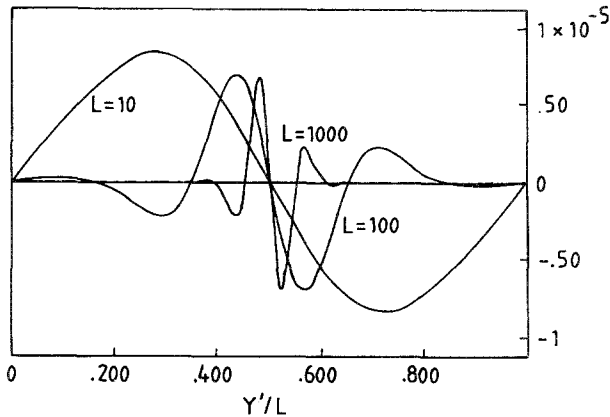

Fig. 4. The nonequilibrium contribution to the correlation function $\langle \delta v(y)\, \delta v(y')\rangle_{st}$ as a function of y/L for $y' = L/2$. The various curves represent various values of the system length L; the other parameters are taken so as to correspond to those used in the computer experiment described in ref. 17 (see caption to Fig. 2).

of the square root of the system size L. This asymptotic result is nicely supported by the numerical evaluations of the corresponding series [see Eq. (16) and Fig. 4]. Although the correlation length is large, the entire function vanishes in the limit of infinite systems.

This is an important result, since it proves that in the presence of a temperature gradient, the existence of the above oscillatory long-ranged correlation function is entirely due to the boundary effects. The same asymptotic behavior is found for the nonequilibrium contribution to the static density autocorrelation function. This, however, is not the case for the density-current static correlation function,[23] since it arises from the broken time-reversal symmetry and is responsible for the asymmetry in the Brillouin lines, even in an infinite medium[9] (see the next section).

These properties of the static correlation functions definitely establish the presence of standing waves across the system generated by fluctuations. They also show the existence of long-range oscillatory correlation functions and the dominant role of the boundary effects on the statistical properties of nonequilibrium systems. From an experimental point of view, the effect is difficult to observe in light scattering measurements, as discussed in ref. 20.

4. SCATTERING FUNCTION IN FINITE MACROSCOPIC SYSTEMS

In this section we study the limiting form of $S_q(\omega)$ appropriate for macroscopic systems. The value of the harmonic number q depends on the wavelength of the incident laser beam used when performing light scattering experiments as well as on the system size L (perpendicular to the incident beam) and the scattering angle. It is customary to express the scattering function in term of the wavenumber K, which is fixed by the characteristics of the experimental setup. Obviously

$$K = 2\pi q/L \tag{20}$$

Typically K is of the order of 10^3–10^5 cm^{-1}, and L is of the order of 1 cm, so that q can take values ranging from a few hundreds to several thousands. In the previous section we derived a limiting form of $S_q(\omega)$, Eq. (14), in the limit of small q. The question is the limit of its validity when q becomes large. Careful analysis shows that the expression (14) remains valid provided

$$q\sqrt{\varepsilon} < O(1) \tag{21}$$

Interestingly, we note that the condition (21) is fulfilled in Beysen's experiments[10] ($K \approx 2 \times 10^3$ cm^{-1}, $L = 0.5$ cm, $\varepsilon \approx 10^{-4}$), so that expression (14) is applicable. The only difference with the molecular dynamic case comes from the fact that now the harmonic number q is large (about 150). As a consequence, we have a fairly large number of finite-size peaks, which now may overlap with the Brillouin lines, giving rise to a spectrum somehow similar to the results of Satten and Ronis.[20] The full discussion of this problem has been given by the above authors and we do not have anything new to add, except perhaps to point out once more the simplicity of our limiting form, Eq. (14), as compared to their results. Note finally that recently Schmitz and Cohen[21] were able to derive a fairly simple form for the integrated spectrum and also discussed the nonlinear effects.

For increasing values of the harmonic number q, the restriction (21) is no longer guaranteed and the expression (14) gradually loses its validity, while at the same time the boundary effects are expected to become less and less important. To study this limit, let us assume that q is large enough so that the following restriction is fulfilled:

$$q\varepsilon > 1 \qquad (22)$$

Then, to dominant order in ε one finds

$$S_K(\omega) \approx \frac{2k_B T_a}{m\pi c^2} \frac{\Gamma/c^2}{(\tilde{\omega}^2 - 1)^2 + 4\tilde{\omega}^2 K^2 \Gamma^2/c^2} \left\{ \left[1 - \frac{1}{L} \frac{c}{\Gamma K^2} (2\tilde{\omega}^2 - 1) \right] \right.$$
$$\left. + \frac{4\gamma}{T_a} \frac{\tilde{\omega}^3 \Gamma/c}{(\tilde{\omega}^2 - 1)^2 + 4\tilde{\omega}^2 K^2 \Gamma^2/c^2} \left(1 - \frac{1}{L} \frac{c}{\Gamma K^2} \frac{3 - \tilde{\omega}^2}{\tilde{\omega}^2} \right) \right\} \qquad (23)$$

If the system size L is much larger than the sound attenuation length $c\Gamma^{-1}K^{-2}$, then the finite-size effects are negligible and the result is precisely the well-known "infinite system approximation" (see, for example, ref. 9). Near the Brillouin peaks ($\tilde{\omega} \approx 1$), the finite-size corrections are strictly negative and as a consequence both the heights and the asymmetry of the peaks are reduced. In most of the equilibrium light scattering experiments[24,30] K is typically of the order of 10^{-5} cm^{-1} and $\Gamma \approx 10^{-3}$ cm^2 sec^{-1}, so that the finite-size correction (height reduction) does not exceed 1 or 2% and so far has not been observed (see ref. 19 for more details). This is not the case for nonequilibrium systems, where the reduction of the asymmetry is indeed an experimental fact.[10–12]

5. CONCLUSION

We have studied the scattering function of a simple fluid under a temperature gradient. By considering a fluid model with vanishing thermal

expansivity coefficient, we were able to derive simple limiting forms for the above function in various limits of interest. In particular, the correction to the usual infinite-system approximation was explicitly derived.

The main purpose of this paper, however, was to understand in terms of simple physics the line shape of the scattering function in very small systems, such as the one realized in computer experiments. The equilibrium theory of light scattering has been developed over the years with very practical considerations in mind, e.g., the possibility of determining important fluid properties; molecular dynamics simulations profit from these results. The nonequilibrium formulation of this theory in finite systems promises to extend the usefulness of this measurement tool. The richness of the spectrum yields a number of independent measures of the static and dynamical properties (e.g., the sound speed and the acoustic damping may be obtained from the Brillouin lines or from any of the standing wave peaks). Interface properties, such as the effective reflection coefficient, may also be studied by the inclusion of more complex boundary conditions, such as accommodating walls or "rough" boundaries.[20,21,31]

We have recently undertaken a systematic study, by computer experiment, of the nonequilibrium dynamical correlation functions in a dilute gas. This effort parallels our earlier work on static correlation functions.[17] Preliminary results exhibit all of the phenomena described above, specifically the presence of the standing wave peaks and a gradient-dependent asymmetry for all of the lines. The oscillatory form of the static velocity–velocity correlation function (Fig. 4) has also been observed.[32] A more complete comparison between our simple model and computer experiments must await the completion of more extensive simulations.[33]

ACKNOWLEDGMENTS

REFERENCES

1. D. Ronis, I. Procaccia, and I. Oppenhein, *Phys. Rev. A* **19**:1324 (1979).
2. D. Ronis and S. Putterman, *Phys. Rev. A* **22**:773 (1980).
3. T. R. Kirkpatrick, E. G. D. Cohen, and J. R. Dorfman, *Phys. Rev. Lett.* **42**:862 (1979); **44**:472 (1980).
4. T. R. Kirkpatrick, E. G. D. Cohen, and J. R. Dorfman, *Phys. Rev. A* **26**:950, 972 (1982).
5. D. Ronis and I. Procaccia, *Phys. Rev. A* **26**:1812 (1982).
6. A. M. Tremblay, M. Arai, and E. D. Siggia, *Phys. Rev. A* **23**:1451 (1981).
7. G. Van der Zwan, D. Bedaux, and P. Mazur, *Physica A* **107**:491 (1981).

8. J. W. Dufty, in *Spectral Line Shapes*, P. Wende, ed. (de Cruger, Berlin, 1981).
9. A. M. Tremblay, in *Recent Developments in Nonequilibrium Thermodynamics*, J. Casas-Vasquez, D. Jou, and G. Lebon, eds. (Springer-Verlag, Berlin, 1984).
10. D. Beysens, Y. Garrabos, and G. Zalczer, *Phys. Rev. Lett.* **45**:403 (1980); D. Beysens, *Physica A* **118**:250 (1983).
11. H. Kiefte, J. M. Clouter, and R. Penney, *Phys. Rev. B* **30**:4017 (1984).
12. G. H. Wegdam, N. M. Keulen, and J. C. F. Michielsen, *Phys. Rev. Lett.* **55**:630 (1985).
13. G. Ciccoti and A. Tenebaum, *J. Stat. Phys.* **23**:767 (1981); A. Tenebaum, G. Ciccoti, and R. Gallio, *Phys. Rev. A* **25**:2778 (1982); A. Tenebaum, *Phys. Rev. A* **28**:3132 (1983).
14. D. J. Evans and W. G. Hoover, *Annu. Rev. Fluid Mech.* **18**:243 (1986).
15. G. A. Bird, *Molecular Gas Dynamics* (Clarendon Press, Oxford, 1976); O. M. Belot-serkovsky, A. I. Erofeyer, and V. E. Yanitsky, in *Numerical Methods in Fluid Dynamics*, N. N. Yanenko and Y. I. Shokin, eds. (Mir, Moscow, 1984).
16. A. Garcia, *Phys. Rev. A* **34**:1454 (1986).
17. M. Malek Mansour, A. Garcia, G. Lie, and E. Clementi, *Phys. Rev. Lett.* **58**:874 (1987); A. Garcia, M. Malek Mansour, G. Lie, M. Mareschal, and E. Clementi, *Phys. Rev. A* **36**:4348 (1987).
18. M. Mareschal and E. Kestemont, *Phys. Rev. A* **30**:1158 (1984).
19. D. Gutkowisc-Krusin and I. Procaccia, *Phys. Rev. Lett.* **48**:417 (1982); *Phys. Rev. A* **27**:2585 (1982), **28**:1602 (1982).
20. G. Satten and D. Ronis, *Phys. Rev. A* **26**:940 (1982).
21. R. Schmitz and E. G. D. Cohen, *Phys. Rev. A* **35**:2602 (1987).
22. L. D. Landau and E. M. Lifschitz, *Fluid Mechanics* (Pergamon Press, Oxford, 1959).
23. M. Malek Mansour, J. W. Turner, and A. Garcia, *J. Stat. Phys.* **48**:1157 (1987).
24. B. J. Berne and R. Pecora, *Dynamic Light Scattering* (Wiley, New York, 1976); J. P. Boon and S. Yip, *Molecular Hydrodynamics* (McGraw-Hill, New York, 1980).
25. T. R. Kirkpatrick and E. G. D. Cohen, *J. Stat. Phys.* **33**:639 (1983); R. Schmitz and E. G. D. Cohen, *J. Stat. Phys.* **38**:285 (1985); **40**:431 (1985).
26. A. Garcia, M. Malek Mansour, G. Lie, and E. Clementi, *J. Stat. Phys.* **47**:209 (1987).
27. P. Resibois and M. De Leener, *Classical Kinetic Theory of Fluids* (Wiley, New York, 1977).
28. T. R. Kirkpatrick and E. G. D. Cohen, *Phys. Rev. A* **26**:995 (1982).
29. A. Rahman and F. Stillinger, *Phys. Rev. A* **10**:368 (1974); R. W. Impey, P. A. Madden, and I. R. McDonald, *Mol. Phys.* **46**:513 (1982); W. E. Alley, B. J. Alder, and S. Yip, *Phys. Rev. A* **27**:3174 (1983); G. C. Lie and E. Clementi, *Phys. Rev. A* **33**:2679 (1986).
30. R. A. Fleury and J. P. Boon, *Phys. Rev.* **186**:244 (1969).
31. G. Satten and D. Ronis, *Physica A* **125**:302 (1984).
32. I. Prigogine, M. Malek Mansour, G. Nicolis, E. Clementi, and G. C. Lie, in *Chemical Processes and Control, Nonlinear Systems* (U. S. Department of Energy, Conf-8605122, 1986).
33. G. C. Lie, A. Garcia, M. Malek Mansour, and E. Clementi, in preparation.